Reconstructing sea level using cyclostationary empirical orthogonal functions

B. D. Hamlington,[1] R. R. Leben,[1] R. S. Nerem,[1] W. Han,[2] and K.-Y. Kim[3]

Received 19 August 2011; revised 22 September 2011; accepted 26 September 2011; published 13 December 2011.

[1] Cyclostationary empirical orthogonal functions, derived from satellite altimetry, are combined with historical sea level measurements from tide gauges to reconstruct sea level fields from 1950 through 2009. Previous sea level reconstructions have utilized empirical orthogonal functions as basis functions, but by using cyclostationary empirical orthogonal functions and by addressing other aspects of the reconstruction procedure, an alternative sea level reconstruction can be computed. The procedure introduced here is capable of capturing the annual cycle and El Niño–Southern Oscillation (ENSO) signals back to 1950, with correlations between the reconstructed ENSO signal and common ENSO indices found to be over 0.9. The regional trends computed from the new reconstruction show good agreement with the trends obtained from the satellite altimetry, but some discrepancies are seen when comparing with previous sea level reconstructions over longer time periods. The computed rate of global mean sea level rise from the reconstructed time series is 1.97 mm/yr from 1950 to 2009 and 3.22 mm/yr from 1993 to 2009.

Citation: Hamlington, B. D., R. R. Leben, R. S. Nerem, W. Han, and K.-Y. Kim (2011), Reconstructing sea level using cyclostationary empirical orthogonal functions, *J. Geophys. Res.*, *116*, C12015, doi:10.1029/2011JC007529.

1. Introduction

[2] Understanding and predicting future sea level change in response to climate change is one of the most important challenges facing climate scientists. Over the past few decades, researchers have used increasingly sophisticated methods to improve monitoring of current ocean conditions and understanding how sea levels will change in the future. A critical question, however, is how the current state of the ocean compares with previous ocean states.

[3] Since 1993, satellite altimetry has provided accurate measurements of sea surface height (SSH) with near-global coverage. These measurements led to the first definitive estimates of global mean sea level (GMSL) rise and have improved understanding of how sea levels are changing regionally at decadal time scales [e.g., *Beckley et al.*, 2007; *Cazenave and Nerem*, 2004; *Leuliette et al.*, 2004; *Miller and Douglas*, 2007; *Nerem et al.*, 2010]. These relatively short records, however, provide no information about the state of the ocean prior to 1993, and with the modern altimetry record spanning only17 years, the lower-frequency signals that are known to be present in the ocean are difficult or impossible to resolve.

[4] Tide gauges, on the other hand, have measured sea level over the last 200 years, with some records extending back to 1807. While providing longer records, the spatial resolution of tide gauge sampling is poor, making studies of the large-scale patterns of ocean variability and estimates of GMSL difficult [e.g., *Douglas*, 1991; *Gröger and Plag*, 1993; *Nerem*, 1995]. The vast majority of tide gauges are located in the Northern Hemisphere, more specifically around the heavily populated areas of North America, western Europe, and Japan, with comparatively few tide gauges located in the Southern Hemisphere. Combining the shorter but essentially complete global coverage afforded by satellite altimetry with the longer but sparsely distributed tide gauge data set is a research area of interest because of the respective shortcomings of tide gauge and satellite altimetry records.

[5] *Chambers et al.* [2002] (hereafter Ch02) made one of the first attempts at combining tide gauge data and satellite altimetry data using a technique known as empirical orthogonal function (EOF) reconstruction. Ch02 removed linear trends from both the tide gauge data and satellite altimetry to focus on capturing the interannual-scale signals such as El Niño–Southern Oscillation (ENSO) and the Pacific Decadal Oscillation (PDO). Although EOF reconstruction was originally developed for use with sea surface temperature (SST) measurements, the method has since been modified for sea level studies, using least squares fitting of satellite altimetry-derived EOFs to the tide gauge data to reconstruct sea levels. Building on this work and that of *Kaplan et al.* [1998, 2000], *Church et al.* [2004] (hereafter CW) produced the most comprehensive and widely cited sea level reconstruction to date, which spans 1950 through 2001. The CW reconstruction, which was later updated [*Church and White*, 2006] to extend back to 1870, has the spatial

[1]Colorado Center for Astrodynamics Research, Department of Aerospace Engineering Sciences, University of Colorado at Boulder, Boulder, Colorado, USA.
[2]Department of Atmospheric and Oceanic Sciences, University of Colorado at Boulder, Boulder, Colorado, USA.
[3]School of Earth and Environmental Science, Seoul National University, Seoul, South Korea.

0148-0227/11/2011JC007529

coverage of satellite altimetry and spans most of the tide gauge record while incorporating trends in the reconstruction. However, only the portion from 1950 through 2001 has been publicly released. While this sea level reconstruction has been cited frequently and used for future sea level projections [e.g., *Church and White*, 2006; *Vermeer and Rahmstorf*, 2009], the fidelity of the reconstructed sea level record is subject to debate. To date, no published and publicly released data set has been produced to improve on the CW method for combining satellite altimetry and tide gauge data, and there has been little discussion regarding deficiencies of the reconstruction.

[6] One primary shortcoming of EOF sea level reconstructions stems from the use of EOFs as basis functions. EOFs decompose a data record into the sum of a set of individual modes composed of a single spatial pattern and a corresponding amplitude time series, which we refer to as the loading vectors (LVs) and principal component (PC) time series, respectively, following the naming conventions of *Kim et al.* [1996]. By definition, the spatial patterns represented by the EOF LVs are time independent (stationary) and only the amplitudes vary in time as described by the PC time series. The spatial patterns of many known phenomena in climate science and geophysics, however, change in time with well-defined periods in addition to fluctuating at longer time scales. Typical responses of a physical system are not stationary but evolve and change over time.

[7] The annual cycle signal in sea level not only oscillates with 1 year periodicity, it also changes amplitude over time, giving rise to a modulated annual cycle (MAC). This and other ocean variability associated with the annual cycle cannot be captured by a single spatial pattern. Similarly, the signal associated with the El Niño–Southern Oscillation (ENSO), which is phase locked to the annual cycle, consists of a quasi-biennial component and a lower-frequency component [*Goswami*, 1995; *Philander*, 1990; *Rasmusson et al.*, 1990; *Rasmusson and Wallace*, 1993]. The biennial component represents phases of El Niño and La Niña, and, like the annual cycle, its amplitude varies over longer time scales.

[8] *Kim et al.* [1996], *Kim and North* [1997], *Kim and Wu* [1999], and *Kim and Chung* [2001] introduced the concept of cyclostationary empirical orthogonal function (CSEOF) analysis to capture the time-varying spatial patterns and longer-time-scale fluctuations present in geophysical signals. The significant difference between CSEOF and EOF analysis is the LVs' time dependence, which allows the spatial pattern of each CSEOF mode to vary in time, with the temporal evolution of the spatial pattern of the CSEOF LVs constrained to be periodic with a selected "nested period." Each CSEOF mode therefore is composed of 12 LVs and one PC time series when using, for example, monthly data and a 1year nested period. This allows the evolution of the annual cycle to be captured in a single mode. In an EOF decomposition, the evolution of the seasonal signal is typically split into several orthogonal computational modes [*Kim and Chung*, 2001], which is one reason the signal is usually removed from the data record by some other means. Recent studies, however, have demonstrated the efficacy of CSEOFs to extract robust modes representing the MAC and ENSO variability [*Trenberth et al.*, 2005; *Hamlington et al.*, 2011]. This leads to the possibility of removing the MAC or ENSO variability from the data without affecting signals associated with other ocean variability.

[9] By using CSEOFs in place of EOFs, it is possible to create an alternative reconstruction, i.e., a reconstruction based solely on EOFs. The motivation for using CSEOFs in place of EOFs is fourfold. EOFs are not an optimal basis for geophysical signals with cyclostationarity (such as the MAC and ENSO). CSEOFs account for the high- and low-frequency components of the annual cycle and do not necessitate the removal of the annual signal from the satellite altimetry or the tide gauge records before reconstruction. Specific signals, such as those relating to the MAC and ENSO that account for the majority of the variability in the altimetric record, can be reconstructed individually using CSEOFs with little mixing of variability between modes. The reconstruction procedure using CSEOFs should also be less sensitive to erroneous tide gauge measurements and poor tide gauge sampling at a given point in time as a result of fitting a larger window of basis functions to the data.

[10] Other considerations, in addition to the choice of basis functions, must be made when attempting to perform the most accurate sea level reconstruction. The reconstruction procedure amounts to solving a weighted least squares problem. The selection of weights can be shown to have a significant impact on the resulting reconstruction. When estimating GMSL from tide gauges, regional clustering of tide gauges needs to be avoided or accounted for in the weighting scheme. A latitudinal-band weighting scheme can be introduced to account for the latitudinal differences in the tide gauge distribution in a similar way to that of *Merrifield et al.* [2009] (hereafter M09). Previous sea level reconstructions do not avoid or account for clustering of the tide gauges, and little discussion has been presented on how this has affected the accuracy of the reconstructions.

[11] In this paper, we propose a modified reconstruction method for combining satellite altimetry data with in situ tide gauge data using CSEOFs as basis functions in the place of EOFs. The structure of this paper is modeled after that of CW. We offer similar validation and comparison, with the added benefit of being able to compare and contrast our CSEOF reconstruction with their EOF reconstruction. We do not compute our own EOF reconstruction for a more direct comparison as the purpose of this paper is primarily to introduce the CSEOF reconstruction technique, and a comprehensive examination of various reconstruction techniques is left for future work. Any areas in which we claim improvement over previous sea level reconstructions are explicitly and specifically stated, and we leave it to future studies, by both ourselves and others, to rigorously test the fidelity of the CSEOF reconstructed data against other sea level data sets. Section 2 of this paper discusses the satellite altimetry data and tide gauge data that we have used for our reconstruction. Section 3 provides an overview of CSEOFs and shows the results of a CSEOF decomposition of the satellite altimetry data. A description of how the reconstruction is performed using CSEOFs is also given in section 3. Section 4 shows the results of the CSEOF sea level reconstruction covering the period 1950 through 2009. The CSEOF reconstruction is compared with other sea level data sets where available. Section 5 gives an evaluation of

the present reconstructions and describes the benefits of the CSEOF reconstruction technique.

2. Data

[12] Both the tide gauge data records and the satellite altimetry data record are required to reconstruct sea levels. The satellite altimetry data is used to find the patterns of spatial variability that will be used as basis functions in the reconstruction procedure. These basis functions are then fit in a least squares sense to the tide gauge records extending back over the time period of interest. Brief descriptions of both the tide gauge and satellite altimetry data sets are given below.

2.1. Tide Gauge Data

[13] The central data set we use for the period 1950 through 2009 is monthly mean sea level records gathered from the data archive at the Permanent Service for Mean Sea Level (PSMSL). We use only the Revised Local Reference (RLR) data, which are measured sea levels at each site relative to a constant local datum over the complete record. At present, we have not included the metric data offered by PSMSL as they can have substantial unknown datum shifts, and their use in time-series analysis is generally not recommended. The data set used from PSMSL was downloaded in August 2010 and contains tide gauge records extending into 2010.

[14] The tide gauges used in the reconstruction are selected with lenient editing criteria. The technique for editing the tide gauges is obtained by the following procedures, similar to those of CW, and the reader is referred to their paper for detailed information on the editing criteria. In summary, we removed tide gauge records of short length and tide gauges with unphysical datum shifts while also editing tide gauges undergoing a month-to-month change of greater than 250 mm. Although the set of tide gauges used in this paper is not identical to that of CW, an effort has been made to produce a data set comparable to the CW tide gauge data set. Some included tide gauges may warrant more careful consideration in the future, but we sought to avoid selectively editing tide gauges, favoring instead to apply the same criteria to every gauge. While it may be appropriate in future studies, we also made no attempt to avoid regional clustering when selecting tide gauge records, resulting in large clusters of tide gauges in Europe, Japan, and North America. We did avoid the use of tide gauges with very short records, instead favoring gauges with good coverage spanning the 60 year record wherever possible.

[15] We linearly interpolated the monthly tide gauge data to weekly intervals to match the 1 week temporal resolution of the altimeter-derived CSEOFs. Prior to this, we filled gaps of 1 to 2 months in the tide gauge records using cubic spline interpolation. We found the nearest grid point for each tide gauge as the basis functions obtained from the satellite altimetry are on a quarter-degree resolution spatial grid. If the nearest grid point was farther than 250 km away, the tide gauge in question was removed from the set. Finally, the available tide gauge records were averaged to produce a single time series if there were multiple tide gauges associated with a single spatial grid point. After the editing procedure, 409 tide gauges remained for use in our reconstruction compared with 426 for CW. The number of available tide gauges through time and the locations of these tide gauges are shown in Figure 1.

[16] The PSMSL sea level data are relative sea levels; therefore the records must be corrected for the ongoing glacial isostatic adjustment. We use the ICE-5G VM2 model. Since an inverted barometer correction is applied to the satellite altimetry data, the sea level measurements from the tide gauges were corrected using an inverted barometer response of sea level to atmospheric loading based on the pressure fields from the National Centers for Environmental Prediction-National Center for Atmospheric Research (NCEP/NCAR) reanalysis.

[17] While most of the editing and preprocessing of the tide gauge records are similar to that used by CW, two significant differences require mention. First, the annual and semiannual cycle signals are not removed from the tide gauge time series prior to performing the reconstruction. One benefit of the CSEOF reconstruction is the ability to account for the MAC in the reconstruction procedure. The second significant departure from the work of CW is that we fit the sea level measurements, not their first derivative, to the LVs used in the reconstruction. Using first derivatives of the tide gauge record is a robust technique to overcome the fact that sea level measurements are made relative to a local datum that varies from one site to another (CW). Fitting CSEOFs to differenced tide gauge time series, however, is significantly more complicated than with EOFs, given the additional time dependence of the CSEOF LVs. In the future we may adopt an approach permitting the use of differenced tide gauge data, but in the present work we just subtract the time mean value from each sea level record. This approach works well when fitting the altimeter-derived CSEOF basis functions, which are constrained to have a periodicity of 1 year. The process of fitting the CSEOF basis functions is found to be relatively insensitive to the small datum shifts or biases that may occur in the edited tide gauges, and the effect of not using differenced data can be minimized by selecting longer tide gauge records covering the majority of the 60 year record that we are reconstructing. Given the considerations above and after conducting some simple tests, we determined that fitting of the CSEOF basis functions to differenced tide gauge data is not required for the 1950–2010 record. This is not likely true when extending the record to earlier than 1950 because the number of available tide gauges varies significantly, thus magnifying the effect of the unknown datum levels. This is the subject of ongoing work and is not discussed at length here. Differencing techniques must be used on the tide gauge records, however, to account for the secular GMSL trend in the reconstruction over the period from 1950 to 2010, as will be discussed in section 3.4.

2.2. Satellite Altimetry Data Set

[18] CSEOF basis functions for our reconstruction were estimated from the Archiving, Validation, and Interpretation of Satellite Oceanographic (AVISO) quarter-degree-resolution, multiple altimeter product based on satellite altimeter measurements spanning 1992–2009 collected by the Topex/Poseidon, ERS-1&2, Geosat Follow-On, Envisat, Jason-1, and OSTM satellites. This updated and reprocessed gridded data product, which was released in June 2010, was created using the delayed time Ssalto/DUACS multimission altimeter data processing system with improved homogenous

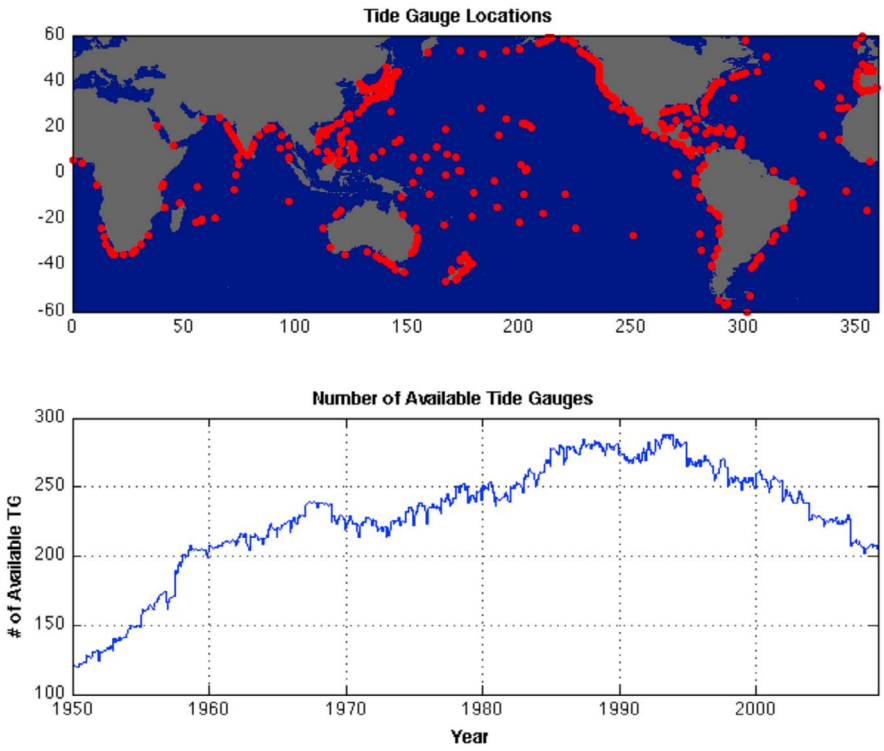

Figure 1. (top) Location of tide gauges used for the reconstruction and (bottom) the number of available tide gauges for use in the reconstruction over time.

corrections and intercalibrations applied to the entire data record. Global crossover minimizations and local inverse methods are used to derive intercalibrated highly accurate along-track data that are referenced to a consistent mean. The along-track data were then merged through a global space-time objective mapping technique that takes into account correlated noise.

[19] We applied very little additional processing other than removing the mean and a linear least squares fit from the time series at each spatial grid point. A CSEOF decomposition of the satellite altimetry data is not able to extract the change in mean sea level into a single mode. It is therefore necessary to remove mean sea level from the satellite altimetry data before computing the basis functions to avoid putting low-frequency power into each CSEOF mode. Although our technique does result in the removal of the spatial pattern of sea level trends, it is unlikely that the regional distribution of sea level trends over the past two decades is the same as that since 1950, and it is therefore unwise to force this stationary pattern on the reconstruction. Removing the trend from each grid point does not significantly affect the ability of the reconstruction to capture decadal time-scale signals. Using the study of *Tai* [1989], the percentage of signal reduction at various periods caused by removing the linear trend from a 17-year record can be computed. Signals with periods of approximately 10 years undergo an RMS signal reduction of less than 5%, and even signals at 20-year periods are reduced by only 30%. Linear detrending of the altimeter data before computing the CSEOFs should therefore have little effect on decadal-scale variations and our ability to capture them in the reconstruction.

[20] The seasonal signal was not removed from the time series prior to computing the CSEOFs. Before CSEOF decomposition, the data were weighted using the square root of the cosine of latitude to yield an area-weighted variance decomposition, grid points at locations with an ocean depth of less than 500 m were removed to mitigate deficiencies in the gridded product associated with measurement and processing errors in shallow water and near the coast, and any grid points without a continuous record over the entire time period were also removed.

3. Methods

[21] Using basis functions computed from a short, spatially dense data set to interpolate a long time series of spatially sparse observations was first implemented in sea surface temperature (SST) studies. *Smith et al.* [1996] computed EOFs from 12 years of satellite-derived SST data and used them as basis functions to estimate global SST temperature fields from 1950 to 1992. *Kaplan et al.* [1998, 2000] improved on this procedure by adding weighting dependent on known errors in the data to the reconstruction procedure. Sea level reconstructions soon followed using the techniques developed for SSTs. The mathematical details are found in the works by *Kaplan et al.* [2000] and CW and thus are not repeated here.

3.1. Previously Published Sea Level Reconstructions

[22] Ch02 computed EOF basis functions from 7 years of satellite altimetry data and used the technique of *Smith et al.* [1996] to create a sea level reconstruction from tide gauges.

Ch02 removed the linear trend and annual signal from both the altimetry and tide gauge data prior to reconstruction. CW also computed basis functions from 7 years of altimetry data, again removing the linear trend, and annual and semiannual signals. However, unlike Ch02, CW accounted for the secular trend in the tide gauge data by adding an artificial constant basis function to the EOFs used in the reconstruction and used the more sophisticated weighting described by *Kaplan et al.* [2000]. Both reconstructed sea levels back to 1950 and neither included the annual signal. The CW reconstruction was later updated [*Church and White*, 2006] and is the most widely cited and available reconstructed sea level data set. Other studies on EOF sea level reconstructions have been published, albeit using data sources other than tide gauges and satellite altimetry or with a more limited scope or region of interest [*Berge-Nguyen et al.*, 2008; *Calafat et al.*, 2009; *Llovel et al.*, 2009; *Christiansen et al.*, 2010]. Furthermore, no published work to date has evaluated (outside of a study by *Christiansen et al.* [2010] on GMSL using simulated data) or attempted to improve on the CW EOF reconstruction technique. Our intent is to focus on the practical issues of combining satellite altimetry and tide gauge data. We have identified three main issues to investigate ways in which the CW reconstruction could potentially be improved: (1) choice of basis functions, (2) selection of weighting scheme, and (3) method of accounting for GMSL.

3.2. Basis Functions: CSEOFs Versus EOFs

[23] When compared with CSEOFs, EOFs have characteristics that make them suboptimal for use as basis functions for sea level reconstruction. EOFs enforce a stationarity on the spatial variability. A single spatial map defines the basis function, and the reconstruction procedure simply computes the amplitude modulation of this map through time. Given the evidence that many signals in geophysical data are cyclostationary, CSEOFs provide significant advantages over EOFs when dealing with signals such as MAC and ENSO signals.

[24] The decomposition of data in terms of a set of basis functions is often very useful in understanding the complicated response of a physical system. By decomposing into less-complicated patterns, it may be easier to understand and shed light on the nature of the variability in a data set. While theoretical basis functions have been studied extensively, exact theoretical basis functions are very difficult to find, and, in general, computational basis functions are sought instead. Perhaps the simplest and most common computational basis functions are EOFs. Consider a simple system defined by:

$$\mathrm{T}(\mathrm{r},\mathrm{t}) = \sum_{\mathrm{i}} \mathrm{LV_i}(\mathrm{r})\mathrm{PC_i}(\mathrm{t}), \tag{1}$$

where LV(r) is a physical process (termed the loading vector, as above) modulated by a stochastic time series PC(t), which is called the principal component time series. Each loading vector and principal component time series pair represents a single EOF mode. As mentioned above, however, physical processes and the corresponding statistics are time dependent, and representing the data with stationary loading vectors can lead to erroneous interpretation of the data.

[25] *Kim et al.* [1996], *Kim and North* [1997], *Kim and Wu* [1999], and *Kim and Chung* [2001] introduced the concept of cyclostationary empirical orthogonal function (CSEOF) analysis to capture the time-varying spatial patterns and longer-time-scale fluctuations present in geophysical signals. The significant difference between CSEOF and EOF analysis is the LVs' time dependence, which allows the spatial pattern of each CSEOF mode to vary in time, with the temporal evolution of the spatial pattern of the CSEOF LVs constrained to be periodic with a selected nested period. In other words, the system is defined as

$$\begin{aligned} \mathrm{T}(\mathrm{r},\mathrm{t}) &= \sum_{\mathrm{i}} \mathrm{LV_i}(\mathrm{r},\mathrm{t})\mathrm{PC_i}(\mathrm{t}) \\ \mathrm{LV}(\mathrm{r},\mathrm{t}) &= \mathrm{LV}(\mathrm{r},\mathrm{t}+\mathrm{d}) \end{aligned} \tag{2}$$

where the loading vectors are now time dependent and are periodic with the nested period d. The CSEOF LVs and corresponding PC time series are obtained by solving:

$$\mathrm{C}(\mathrm{r},\mathrm{t};\mathrm{r}',\mathrm{t}')\mathrm{LV_n}(\mathrm{r}',\mathrm{t}') = \lambda_{\mathrm{n}}\mathrm{LV_n}(\mathrm{r},\mathrm{t}), \tag{3}$$

with r' and t' representing other points in space and time, respectively, and under the assumption that:

$$\mathrm{C}(\mathrm{r},\mathrm{t};\mathrm{r}',\mathrm{t}') = \mathrm{C}(\mathrm{r},\mathrm{t}+\mathrm{d};\mathrm{r}',\mathrm{t}'+\mathrm{d}). \tag{4}$$

[26] In other words, the space-time covariance function is periodic in time with the nested period d. Since the covariance matrix cannot be written as a square matrix, equation (3) cannot be solved in the same manner as EOFs. Instead, equation (3) is Fourier transformed twice with respect to t and t', making use of the assumption that the covariance matrix is periodic. Because of the periodicity of the covariance function, equation (3) can be written in the same form as EOFs in Fourier space. The PC time series in Fourier space are easy to obtain, and, finally, both the LVs and PC time series are transformed back to physical space. For further details, the reader should refer to the work by *Kim et al.* [1996] in which a detailed description of the computation of CSEOFs is provided.

[27] When focusing on the annual and ENSO signals, the nested period is defined to be 1 year. *Hamlington et al.* [2011] have demonstrated the ability of CSEOF analysis with a nested period of 1 year to extract MAC and ENSO signals from the AVISO satellite altimetry data. Figures 2 and 3 show CSEOF modes 1 and 2 computed from 17 years of the AVISO multisatellite altimetry data. These two modes capture the MAC and ENSO signals, respectively, and account for nearly 50% of the sea level variability. For the weekly AVISO data, 52 separate LVs are obtained for each mode (only 12 interpolated monthly LVs are shown in Figures 2 and 3 in the interest of conserving space), with the PC time series representing the amplitude modulation of these LVs over time.

[28] The 1 year periodicity associated with the annual cycle is not seen in the PC time series of mode one (Figure 2), but instead is contained in the 12 LVs shown. Figure 2b shows the annual cycle contribution to GMSL calculated by combining the mode 1 LVs and PC time series according to equation (3), with only the annual cycle mode used. The

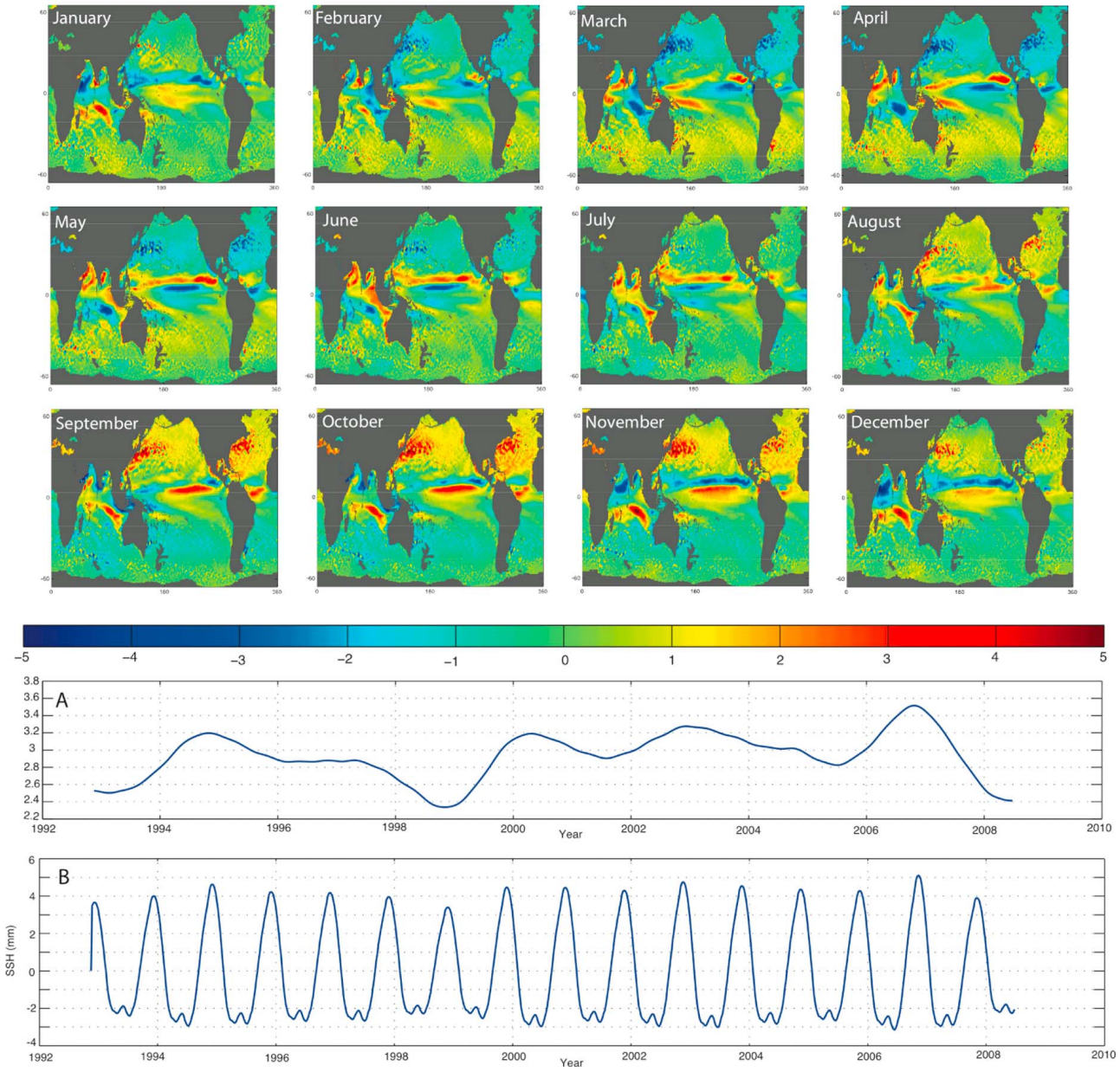

Figure 2. CSEOF mode 1 captures the modulated annual cycle (MAC). The plots show the mode 1 monthly time-dependent LVs (color images), (a) the PC time series, and (b) the reconstructed mode 1 contribution to global mean sea level (GMSL).

1 year cycle and its lower-frequency modulation are apparent, and one begins to appreciate how a CSEOF mode is both similar to and different from an EOF mode. Additionally, as a result of the relationship between the annual cycle and ENSO signal, a 1 year nested period results in a mode directly linked to the ENSO variability in the satellite altimetry data (Figure 3). Only19 CSEOF modes are needed to explain 95% of the variance in the altimetric record. The first five modes explain 34%, 17%, 8%, 6%, and 5% of the variance in the detrended AVISO data. When performing sea level reconstructions, every LV space-time pattern associated with an individual CSEOF mode is fit simultaneously, which reduces the sensitivity of the resulting reconstruction to the sampling error associated with the limited number of tide gauge measurements and to erroneous tide gauge measurements at a single point in time. In other words, rather than fitting a single spatial pattern at a single point in time as in an EOF reconstruction, we fit a window of 52 spatial patterns to 52 points in time. This allows more robust reconstructions to be produced when compared with reconstruction techniques using EOF basis functions.

[29] The MAC signal is well captured by the first CSEOF mode and there is no leakage into the second mode, which is associated with ENSO variability in the altimetry record (illustrated in Figures 2 and 3). On the other hand, when performing EOF decomposition, the annual cycle signal is spread across several computational modes, which is a well-known issue with EOF analysis [*North*, 1984; *Kim and Wu*,

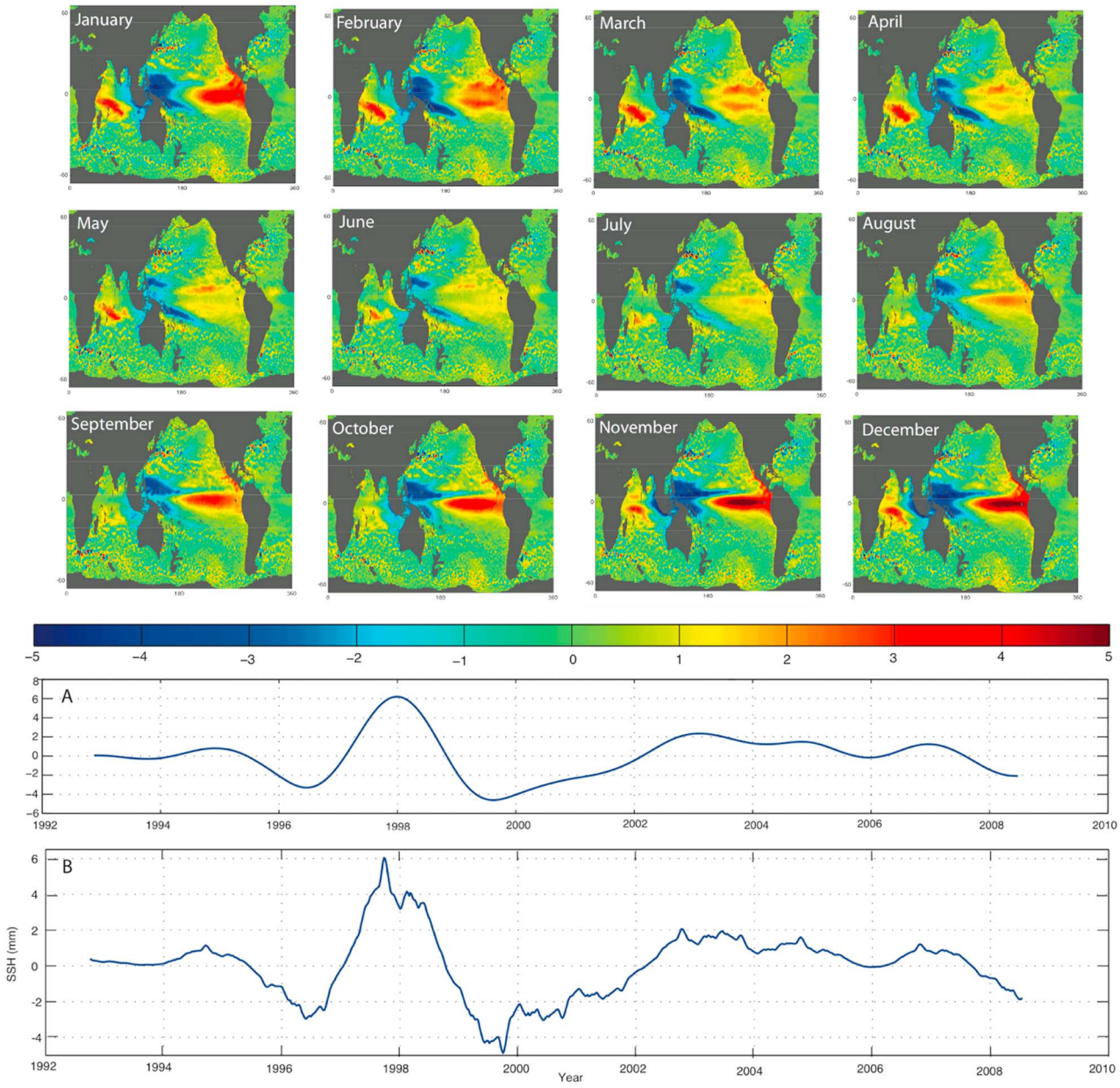

Figure 3. CSEOF mode 2 captures ENSO. The plots show the mode 2 monthly time-dependent LVs (color images), (a) the PC time series, and (b) the reconstructed mode 2 contribution to global mean sea level (GMSL).

1999; *Kim and Chung*, 2001]. Therefore, CSEOF basis functions allow for the reconstruction of specific signals, such as those attributed to the MAC or ENSO. More important, if a CSEOF mode can be physically interpreted and identified as belonging to a certain climate or geophysical process, the mode can be used as a basis function to reconstruct that process back in time. This has important implications for climate monitoring and allows for the possibility of estimating the MAC or ENSO signal dating back to the earliest tide gauge measurements. EOF basis functions, on the other hand, do not separate physical processes nearly as well, making it more difficult to reconstruct cyclostationary signals. In the Ch02 and CW sea level reconstructions, the annual and semiannual cycle signals are removed from both the satellite altimetry data and tide gauge data prior to performing the reconstruction.

[30] *Christiansen et al.* [2010] discussed the implications of the length of the time series available for computing basis functions on the resulting sea level reconstruction. It was concluded that longer calibration periods lead to better reconstructions, and for shorter calibration time periods (similar to the length of the satellite altimetry data) an extra basis function must be included to capture the GMSL. To test the ability of the CSEOF technique to extract meaningful patterns from the satellite altimetry data, *Hamlington et al.* [2011] performed CSEOF decompositions on 4, 8, 12, and

16 years of satellite altimetry data. Only after a 8 year record was available did an ENSO-related CSEOF mode become physically interpretable, and even with a 16 year record, the GMSL time series and regional distribution of sea level trends could not be extracted in a single CSEOF mode. The inability of either EOFs or CSEOFs to capture the secular trend from such a short calibration period leads directly to the conclusion by *Christiansen et al.* [2010] that some other method must be used in the reconstruction procedure to capture GMSL and the spatial pattern of the secular trend when only a short calibration time period is available. We do not attempt to compute sea level reconstructions with differing lengths of the calibration period, but in light of the conclusions by *Christiansen et al.* [2010] and *Hamlington et al.* [2011], we acknowledge that any calibration period shorter than the 17 years used here would lead to an inferior reconstruction. Furthermore, a length greater than 17 years would likely lead to an improved reconstruction, but this has no practical consequence for our goal of computing the best possible sea level reconstruction using satellite altimetry and tide gauge data at this time. Significantly reducing the calibration period would also make comparisons difficult because of the substantial change in CSEOF basis functions that would occur [*Hamlington et al.*, 2011]. We could choose to determine the CSEOFs from numerical model results, but ideally the CSEOF reconstructed sea level data presented here could be used to test model results, and we thus seek to obtain an independent assessment of sea level back to 1950.

3.3. Weighting Scheme

[31] In addition to the choice of a basis function, careful consideration must be given to the weighting scheme used in the reconstruction procedure since the amplitudes of each basis function are calculated by solving a weighted least squares problem. *Kaplan et al.* [2000] and CW utilize truncation and measurement errors for weighting, while *Smith et al.* [1996] and Ch02 omit weighting. As discussed by M09, the sparse spatial distribution of the tide gauges must be taken into account to get a meaningful estimate of GMSL from tide gauges. Although regional clustering around heavily populated areas can be avoided by careful selection of tide gauges, it is difficult to account for the latitudinal differences in the number of tide gauges used in the analysis. There are many more tide gauges in the Northern Hemisphere when compared with those of the Southern Hemisphere, and weighting each tide gauge equally would lead to a reconstruction strongly biased by Northern Hemisphere signals. In their paper, M09 show the disparity between GMSL trends in the Southern Hemisphere versus the Northern Hemisphere over the last 50 years. For this reason, a more appropriate weighting may be one similar to the one M09 employed that uses weights inversely proportional to the number of tide gauges in each 10° latitude band while also accounting for the relative differences in ocean area contained in each band. This weighting scheme should lead to a more accurate sea level reconstruction and a more accurate estimate of GMSL and has thus been selected for the CSEOF reconstruction presented here.

3.4. GMSL

[32] Estimating GMSL using reconstruction techniques is not a trivial task. *Christiansen et al.* [2010] discussed the difficulties of estimating GMSL using EOF reconstruction techniques, albeit using model data instead of satellite altimetry and tide gauge data. While CSEOF basis functions describe the cyclostationary variability in sea level, as a result of the short length of the satellite altimetry record, no single CSEOF mode captures the secular trend. EOF analysis of the satellite altimetry record has similar difficulties in extracting the secular trend. Even if the CSEOF analysis were capable of extracting the secular trend from the AVISO data, we cannot assume that the resulting spatial pattern is stationary over the entire 60 year time period. CW approximate the trend in their reconstruction by introducing a constant basis function that is fit along with the other EOF basis functions. As shown by *Christiansen et al.* [2010], fitting this constant basis function produces a result that is very similar to computing a weighted average of the sea level measured by the tide gauges at each point in time. The spatially uniform basis function distributes this same time series to every spatial point in the reconstruction. This leads to mean sea levels being very similar when values are averaged independently over the Northern and Southern Hemispheres, which contradicts the tide gauge analysis of hemispheric mean sea level presented by M09. The CW method of handling GMSL also does not account for sampling biases caused by the sparse distribution of tide gauges. In other words, GMSL will be biased toward areas with large numbers of tide gauges and will be more representative of mean sea level in these areas than the actual GMSL. On a global scale, each of the reconstructed CSEOF modes has a small secular trend. However, when sampled at the tide gauge locations and with uneven sampling through time, the individual modes could contribute significant trends to GMSL. Regardless, when using a constant basis function, it is difficult to obtain more information than is contained in the tide gauges regarding GMSL by performing a sea level reconstruction. The constant basis function is completely independent of the altimeter record, and thus there is no implicit optimality in its functional form as would be the case for an EOF or CSEOF pattern derived from satellite altimetry.

[33] Rather than introducing an additional basis function in an attempt to account for the secular trend as CW did, we separate the computation of the secular trend from the actual reconstruction procedure. By secular trend, we refer not only to the linear portion of the trend, but also to the nonperiodic variations that are unexplained by the reconstruction computed using the CSEOF basis functions. The altimetry-derived CSEOF basis functions are insensitive to the secular trend in the tide gauges largely because of the annual nested periodicity imposed on the spatial and temporal variability of the relatively short altimetric record. Separating the computation of the trend from the reconstruction computation is also necessary because of the complexity of implementing a CSEOF reconstruction with differenced tide gauge data. The time dependence of the LVs would introduce a term in the least squares procedure necessitating the computation of the time derivative of the LVs. While possible, this is an unnecessary complication for the work presented here and a topic we leave for future research. Therefore, the following procedure is used to estimate GMSL:

[34] 1. The full CSEOF reconstruction is computed and re-formed into a data set as given by equations (2). This data set is then subsampled at each of the tide gauge locations.

This provides a reconstructed sea level time series including signals such as ENSO from 1950 to 2009 at each of the tide gauge locations.

[35] 2. The time series from part 1 are differenced for each tide gauge location. The differenced time series are ensemble averaged at each point in time using latitude-band weighting and finally reintegrated (first differences of the tide gauge data are used to mitigate the lack of a consistent datum for the tide gauges). This provides a time series from the averaged CSEOF reconstruction that has been subsampled at each tide gauge location. This time series contains signals such as the MAC and ENSO and indeed any signal that our reconstruction captures but not the secular trend contained in the raw tide gauge data.

[36] 3. The raw tide gauge data are also differenced, averaged using latitude-band weighting at each point in time, and then reintegrated to form a time series associated with the original tide gauge data. This time series will include the secular trend in the tide gauge data as well as the MAC, ENSO, and other ocean signals contained in the raw tide gauge data.

[37] 4. The time series computed in part 2is subtracted from the time series computed in part 3 to form an estimate of the secular trend in the tide gauge data with all reconstructed signals removed, including MAC and ENSO signals,

$$\mathrm{Trend_{TG}} = \overline{\mathrm{TG_{raw}}} - \overline{\mathrm{Recon_{TG}}}, \tag{5}$$

where $\overline{\mathrm{TG_{raw}}}$ is the average of the original tide gauge data, $\overline{\mathrm{Recon_{TG}}}$ is the average of the reconstruction at the tide gauge locations, and $\mathrm{Trend_{TG}}$ is the estimate of the secular trend with reconstructed signals removed. This process corrects for any trend resulting from the spatial subsampling of signals captured by the reconstruction and removes variability resulting from signals such as the MAC and ENSO.

[38] 5. Finally, GMSL can be computed by adding the time series $\mathrm{Trend_{TG}}$ computed in part 4 to the time series obtained by globally averaging the CSEOF reconstructed data:

$$\mathrm{GMSL} = \overline{\mathrm{Recon}} + \mathrm{Trend_{TG}}. \tag{6}$$

GMSL contains the secular trend from the tide gauge data as well as the MAC and ENSO signals captured by the reconstruction.

[39] In short, we have used the CSEOFs to estimate the MAC and ENSO (and other interannual signals) and then removed this variability from the weighted average of the tide gauge data. The resulting time series is then added back into the reconstruction, and the GMSL time series (including signals such as ENSO) is computed by averaging the CSEOF reconstruction globally at each point in time. This procedure is similar to that used by *Hamlington et al.* [2011] with the goal of removing explainable variability from a time series. This should result in an improved signal-to-noise ratio and thus an improved estimate of the trend in GMSL. The $\mathrm{Trend_{TG}}$ time series computed by this method is not directly comparable to that provided by CW or AVISO as it does not include signals such as ENSO. However, the trend values computed from $\mathrm{Trend_{TG}}$ should be superior to the trends computed from GMSL estimated in part 5 since more of the variability has been explained and removed prior to calculation, thus improving the error bars in our estimate of the secular trend in GMSL.

4. Results

[40] With the considerations outlined above, a CSEOF sea level reconstruction for 1950–2009 has been computed using latitude-band weighting and a set of tide gauges obtained using editing criteria very similar to that described by CW. An inverse barometer correction was applied to both the tide gauge data and the altimetry, and no attempt was made to remove the annual cycle signal. The basis functions for the reconstruction are given by a CSEOF decomposition of the AVISO merged satellite altimetry data spanning the period 1993 through 2009. Before decomposition, the time series at each grid point was detrended by removing a least squares fit linear trend, and the resulting value was area weighted by multiplying by the square root of the cosine of the latitude to yield an area-weighted variance decomposition. A nested period of 1 year was used to capture the variability associated with MAC and ENSO. While other (longer) nested periods could be used, a 1 year nested period robustly captures the MAC and dominant ENSO signal in the first two CSEOF modes (Figures 2 and 3). The 19 leading CSEOF modes describe 95% of the variability in the original data set. Once obtained, these 19 CSEOF modes are used as basis functions and fit to the tide gauge data using weighted least squares. To justify the use of all 19 modes, a test similar to that outlined by CW is conducted. We use the F test and find that the reduction in variance is significant at the 95% confidence level (many modes are significant at the 99% level) for each mode other than modes 10 and 14, which are significant at the 90% confidence level, and mode 15, which actually leads to a slight increase in variance. By fitting a larger window (52 points in time) in the case of the CSEOF reconstruction, overfitting should be more effectively avoided when compared with an EOF reconstruction. In general, a single CSEOF mode should also describe more variance than a single EOF mode without increasing the degrees of freedom as the spatial patterns in an individual CSEOF mode are not independent. CW fit 20 EOF modes but do state that it would be equally justifiable to fit 10 or 30 EOF modes. Results obtained using the reconstructed data set computed with all 19 CSEOF modes are described below.

4.1. Comparison With Altimetry

[41] Since the LVs for the AVISO satellite altimetry CSEOF decomposition and the reconstructed data set are identical, the goal of our work is to reproduce the PC time series associated with each LV (basis function) back through time using the tide gauges. The tide-gauge-reconstructed PC time series for the first five CSEOF modes are shown in Figure 4 overlaid with the original altimeter-derived PC time series. The quality of the reconstruction is clearly seen by the close agreement between the two. The first mode captures the MAC and the result is stable back to 1950, demonstrating the significant advantage of the CSEOF method versus sea level reconstructions computed using EOF basis functions without the annual cycle. The second mode in Figure 4 captures ENSO. The correlation between tide-gauge-reconstructed and altimetry PC time series is 0.97 between

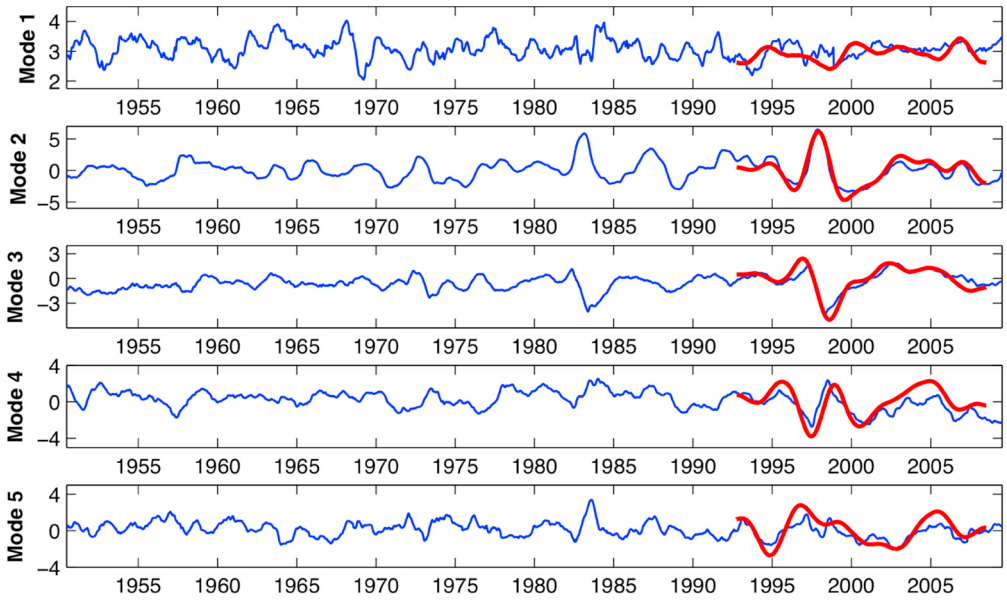

Figure 4. Reconstructed amplitudes computed for the first five CSEOF modes (blue). The first mode is associated with the annual cycle while the second mode is associated with the ENSO signal. The CSEOF PC time series (red) computed from the altimetry data are also plotted and are seen to have excellent agreement with the computed amplitudes.

1993 and 2010. Similarly, modes 3, 4, and 5 have correlations of 0.94, 0.82, and 0.67, respectively, over the same time period. These high correlations demonstrate the ability of the CSEOF reconstruction method to estimate modes from sparse tide gauge samplings that agree very well with the modes derived from satellite altimetry.

[42] While the comparison of the PC time series arising from the reconstruction and CSEOF decomposition of the satellite altimetry gives an indication of the quality of the reconstruction, there is a direct comparison between the reconstructed sea level data and the AVISO satellite altimetry data. The regional trends over the period 1993–2009 are computed for both the AVISO data (Figure 5a) and the CSEOF reconstruction data (Figure 5b). We observe good agreement between the two trend maps, particularly in the Pacific and Atlantic oceans. The main area of disagreement between the two maps is found in the Indian Ocean. This is likely a result of the reduced availability of tide gauge data in the PSMSL data set in the Indian Ocean after 2000 (see Figure 1). The spatial distribution of the correlation between the CSEOF reconstruction and AVISO data (Figure 5c) over the 17 years from 1993 to 2009 has a global area-weighted average of 0.68, with much higher correlations in the tropics. The annual cycle is removed from both the AVISO data and CSEOF reconstruction prior to computation of Figure 5c to avoid simply correlating the annual cycle signal. As noted by CW, the higher correlation in the tropics reflects the dominance of the low-order basis functions that contain the variability associated with the large-scale signals in the data. The correlations found in the northern Pacific Ocean and Atlantic Ocean using the CSEOF reconstruction are markedly higher than those found from the EOF reconstruction of CW, suggesting that CSEOFs better capture the ocean variability in those regions.

4.2. Comparison With Other Sea Level Data

[43] As with any new technique, it is important to compare how the new results compare with results obtained from previous techniques. The CW data set spanning the period 1950–to 2001 is publicly available through the PSMSL website and can be used for comparison with our CSEOF reconstructed sea level data. CW use TOPEX/Poseidon satellite altimetry data from 1993 through 2001 to compute their basis functions. Their reconstructed data compare favorably with the satellite altimetry data over this time period. As expected, the trends computed from the CSEOF reconstruction from 1993 to 2001 (Figure 6a) show good agreement with the CW trends over the same period (Figure 6b). The trends in the Indian Ocean also show good agreement, further suggesting that the disagreement between the CSEOF reconstruction and AVISO data is a result of reduced tide gauge data availability after 2000. When comparing the trends computed from 1950 to 2001, however, there is little agreement between the spatial variability of the trends computed from the CSEOF reconstruction (Figure 6c) and the CW reconstruction (Figure 6d). This could be a result of the different basis functions, different tide gauge set, and/or different weighting scheme. Since these data sets are the only two available sea level reconstructions, it is difficult to determine which is more accurate without independent comparisons.

[44] In a recent paper, *Han et al.* [2010] identified the spatial pattern of sea level changes in the Indian Ocean since the 1960s by analyzing independent oceanographic and atmospheric data sets, performing model experiments using ocean general circulation models (OGCMs) and atmospheric GCMs, and analyzing coupled global climate model solutions. They suggested that the spatial pattern of sea level

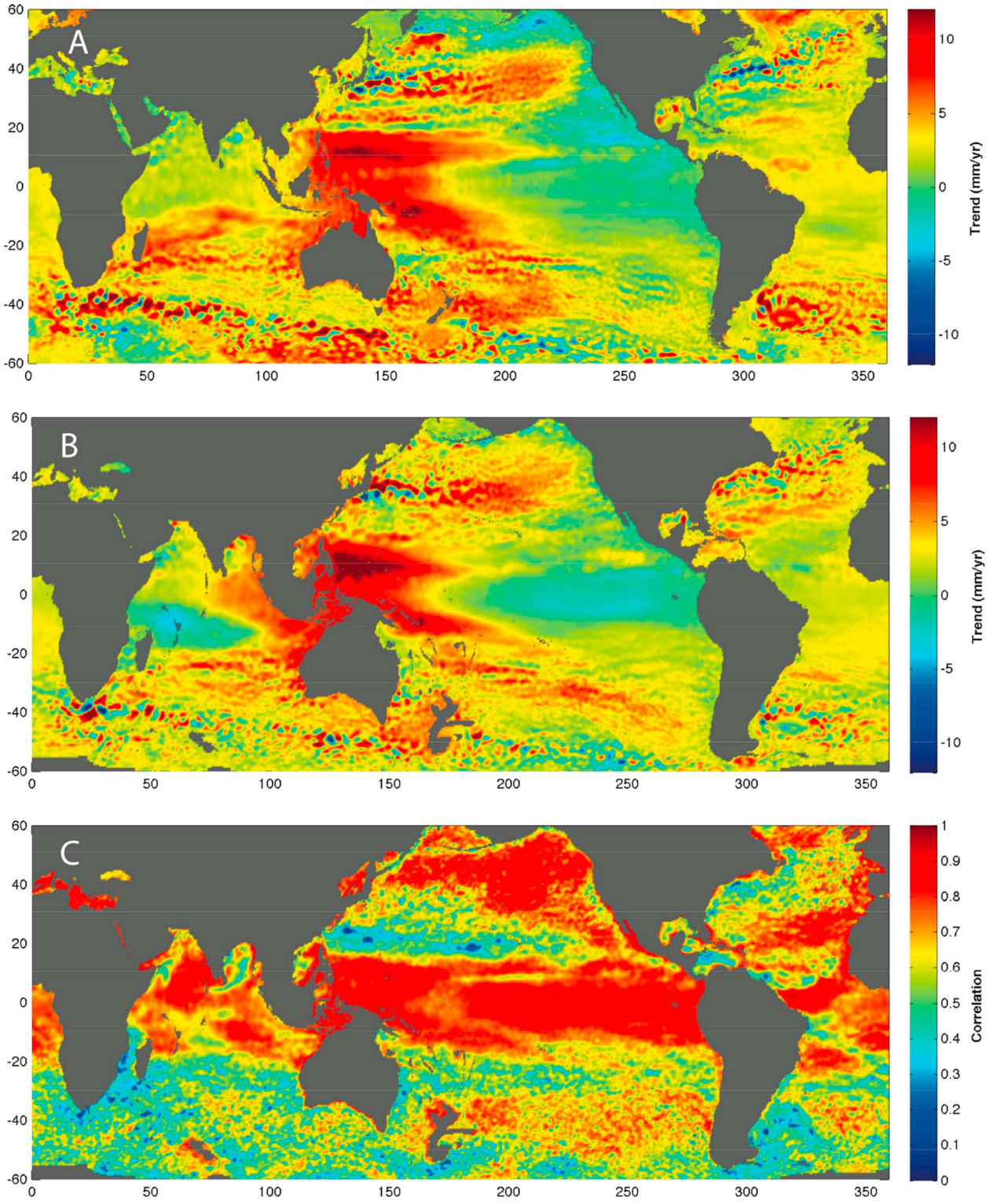

Figure 5. Regional sea level trends from 1993 to 2009 computed from (a) the AVISO satellite altimetry data and (b) the CSEOF reconstruction. (c) The spatial variation of correlation between the AVISO and CSEOF reconstruction data over the same time period is also shown. Note that the annual cycle has been removed from both the AVISO data and reconstruction prior to computing Figure 5c.

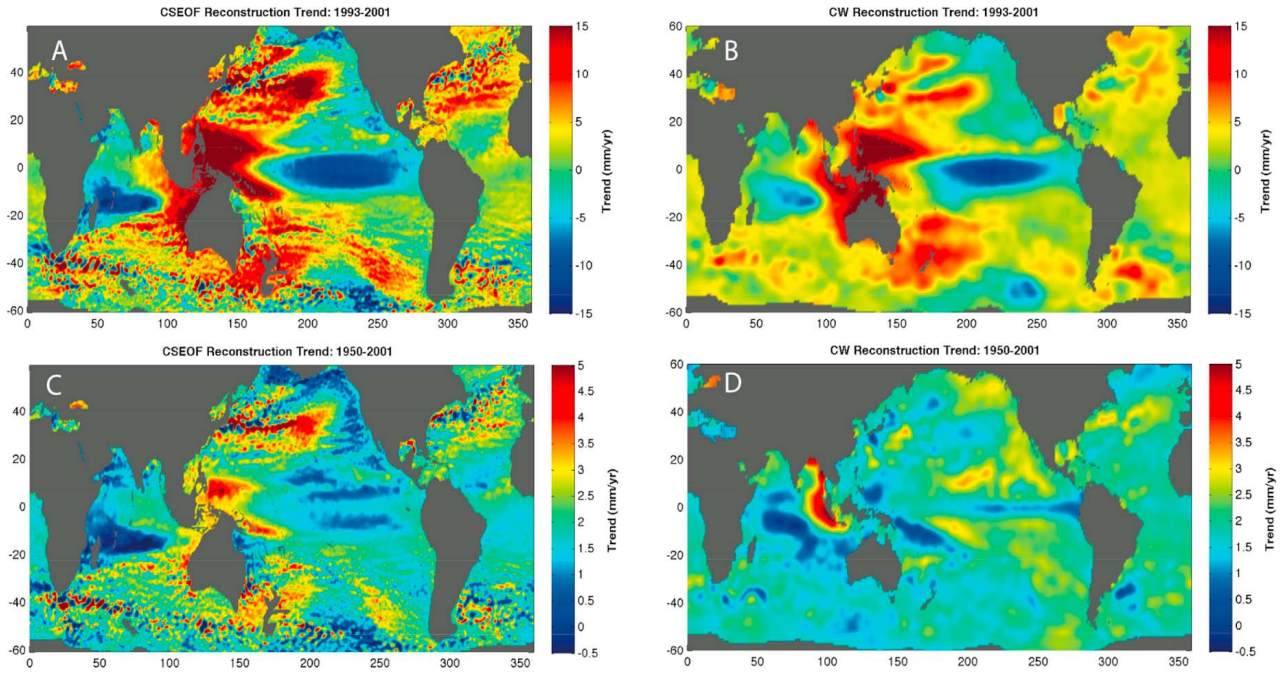

Figure 6. Regional sea level trends from 1993 to 2001 computed from (a) the CSEOF reconstruction and (b) the CW EOF reconstruction, and from 1950 to 2001 computed from (c) the CSEOF reconstruction and (d) the CW EOF reconstruction.

change is robust to cross-data sampling and cross-model differences and agrees well with tide gauge and satellite observations during their overlapping periods. Sea level trends computed from the CSEOF reconstruction for the period of 1961–2001 agree better with the *Han et al.* [2010] trends than with the CW reconstruction in the south Indian Ocean (Figure 7). The spatial structure and extent of the sea level fall in the south tropical Indian Ocean, and the sea level rise north and west of Australia, which are also shown in the tide gauge data [*Han et al.*, 2010, Figure 1], as well as the sea level rise in the subtropical south Indian Ocean, are more faithfully reproduced by the CSEOF reconstruction. In the Bay of Bengal and southern subtropical ocean, the CSEOF data appear to underestimate the sea level rise more than the CW data. As noted in the supplementary information by *Han et al.* [2010], however, the model most likely overestimates the trend in the southern subtropical ocean so the disagreement seen in the region is not surprising. Regardless, this independent validation of the CSEOF reconstruction from 1961 through 2001 suggests that the CSEOF-based technique likely provides more accurate estimates of sea level trends from 1950 to 2009 when compared with past sea level reconstructions at least for the dominant trend signal in the Indian Ocean.

4.3. ENSO

[45] ENSO is described by CSEOF mode 2 in both the satellite altimetry (Figure 3) and the reconstructed sea level (Figure 4). A variety of indices are used to monitor ENSO. One commonly cited index is the Multivariate ENSO Index (MEI). The MEI is computed using six different variables, but does not include SSH measurements [*Wolter*, 2010; *Wolter and Timlin*, 1998]. In Figure 8, the reconstructed ENSO mode is shown along with the MEI for the period 1950 to 2009. The correlation between the MEI and the reconstructed ENSO (mode 2) is 0.91. Although CW found a single EOF mode related to ENSO, the correlation between their reconstructed amplitude and the Southern Oscillation Index (SOI) was only 0.78 over from 1950 to 2000, underlining the ability of the CSEOF-based technique to better reconstruct the ENSO signal back in time.

[46] While a single CSEOF mode captures the signal represented in common ENSO indices, it is unlikely that this is the entirety of the signal. Recent studies suggest that ENSO cannot be explained by a single index or mode, but is better defined as a set or series of dynamical modes [*Compo and Sardeshmukh*, 2010]. By using CSEOFs, it is likely that we are capturing the traditional eastern Pacific ENSO dynamical signal in a single mode; however, initial reconstructions also suggest that higher-order modes may explain other components of the ENSO signal. The third CSEOF mode in Figure 4 appears to capture the ENSO Modoki signal [*Ashok et al.*, 2007], judging by the spatial pattern of the LVs and also because this mode has a correlation of 0.55 with an El Niño Modoki SST index from 1950 to 2010. Further analysis is needed of the higher-order modes to gain a more thorough understanding of their physical basis.

4.4. Global Mean Sea Level

[47] The trend in Trend_{TG} (equation (5)) from 1950 to 2009 is estimated to be 1.97 mm/yr (Figure 9), using the CSEOF reconstruction and the technique outlined in section 3.4. Meanwhile, the subsampled reconstruction accounts for 0.08 mm/yr of the GMSL trend at the tide gauge locations. Without correcting for the sampling bias using the reconstruction, a trend of 2.03 mm/yr is found using latitude-band weighting of the tide gauges. For comparison, CW estimate the trend in GMSL to be 1.8 mm/yr from 1950 through 2001

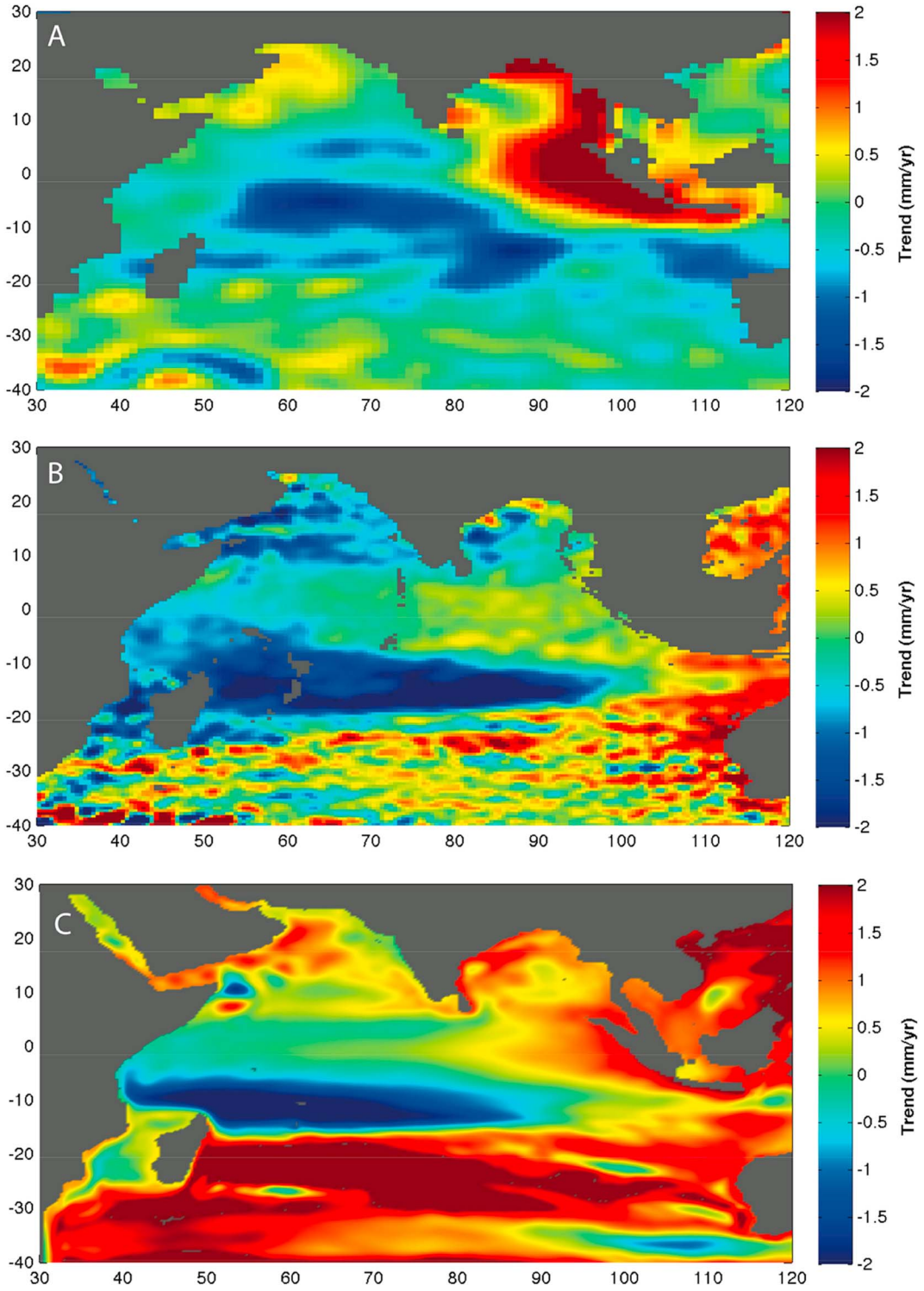

Figure 7. Regional sea level trends from 1961 to 2001 computed from (a) the CW EOF reconstruction, (b) the CSEOF reconstruction, and (c) from the Hybrid Coordinate Ocean Model solution of *Han et al.* [2010]. Note that different bathymetry editing was applied to the data sets used to compute the three figures above.

with the trend from the CSEOF reconstruction computed to be 1.90 mm/yr over the same period. While the two estimates of the trend in GMSL show good agreement, the variability in each of the GMSL time series is substantially different. This could be a result of differences in the tide gauge data, but more likely represents the differences that occur from the reconstruction correction that is made in the case of our CSEOF reconstruction GMSL estimate.

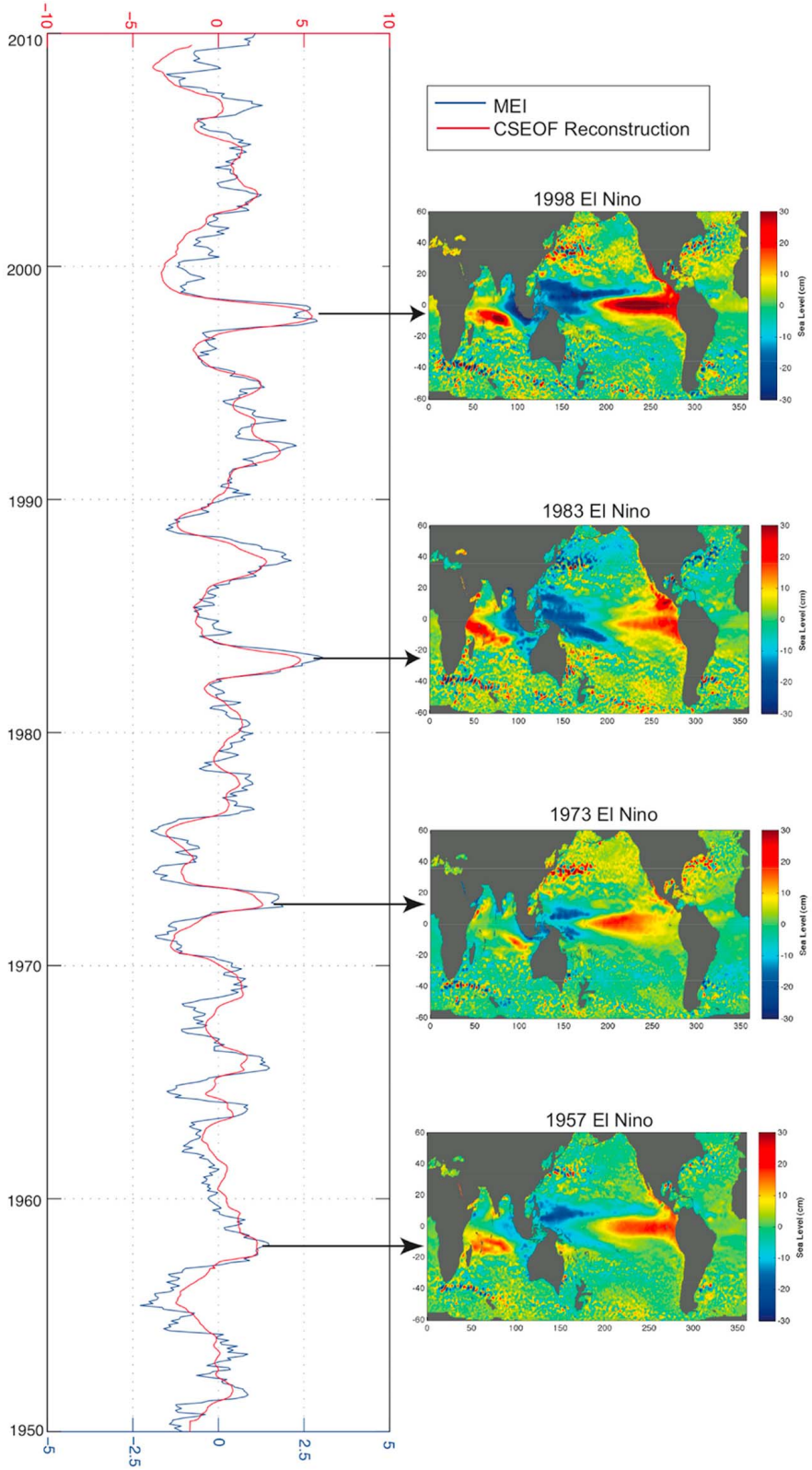

Figure 8. ENSO SSH index calculated from reconstructed CSEOF mode 2 (red line) compared with MEI (blue line) from 1950 to 2009. The spatial maps of sea level for four significant El Niño events over the 60 year record are also shown.

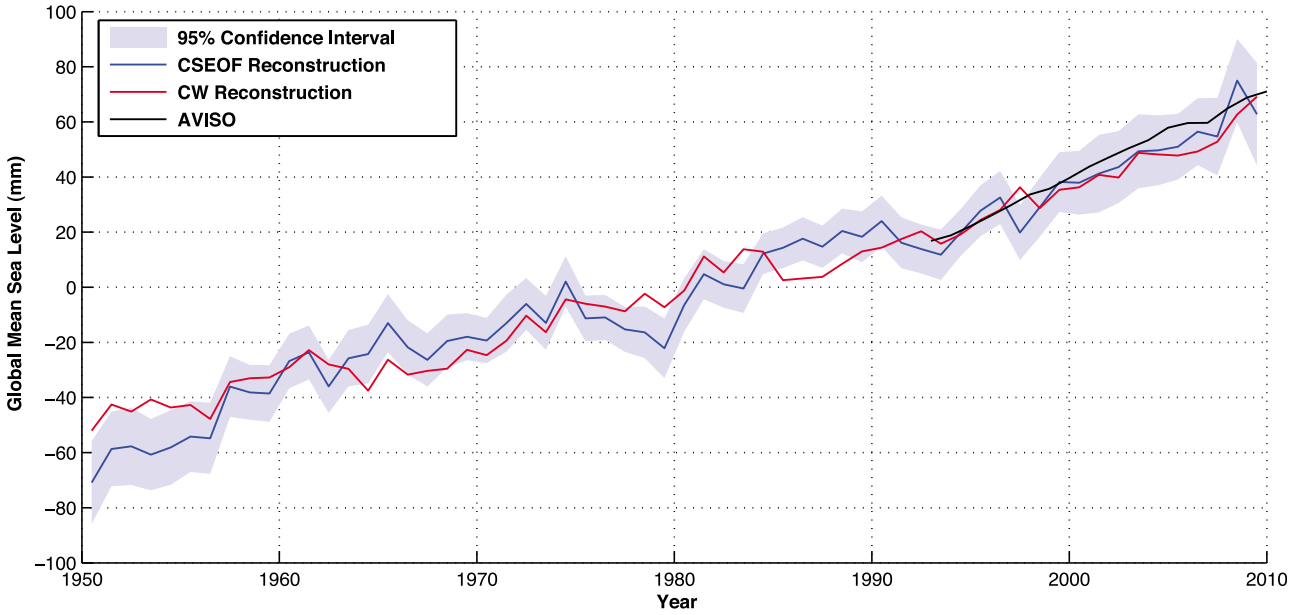

Figure 9. A comparison of GMSLs derived from satellite altimetry (1993–present; black) from the CSEOF reconstruction using latitudinal-band weighting (blue) and from the CW EOF reconstruction (red).

[48] The trend in Trend_{TG} (equation (5)) from the CSEOF reconstruction technique is estimated to be 3.22 mm/yr from 1993 to 2009. The subsampled reconstruction accounts for an additional 0.04 mm/yr of GMSL trend at the tide gauge locations. For comparison, the GMSL estimated from the AVISO satellite altimetry data is 3.28 mm/yr, again showing good agreement with the reconstructed GMSL.

[49] While it is difficult to obtain a formal estimate of the error in the GMSL trend, we can use a randomization procedure to determine the sensitivity of the trend to the tide gauge selection. The sensitivity was estimated using a Monte Carlo procedure in which only 70% of the total available tide gauges were used for the reconstruction. The entire reconstruction procedure was carried out (including the correction of GMSL) 100 times, and the statistics were computed from the results. The 95% confidence interval on the Trend_{TG} time series is shown in Figure 9. The reconstruction itself was relatively insensitive to the tide gauge selection. The ENSO mode correlation with the MEI was found to be 0.90 ± 0.04 across the 100 trials. On the other hand, the GMSL estimates were much more sensitive to selection of tide gauges. Over the period 1950–2009, the estimate of the trend in GMSL was 1.95 ± 0.4 mm/yr across the 100 trials. Furthermore, the estimate of the trend in GMSL from 1993 to 2009 was 3.52 ± 0.6 mm/yr. These standard deviations are much larger than those found by CW using similar randomization tests. This increased sensitivity likely results from the use of latitude-band weighting. If a given 10° latitude band contains only two tide gauges at a certain time, removing one of these will have a significant effect on the estimate of GMSL since each latitude band is weighted equally. This effect is more pronounced at the ends of the time series, where the total number of tide gauges available is smaller. While this may be one advantage of using other weighting or even non-weighting schemes to compute GMSL, we are encouraged by the robustness of our reconstruction with latitude-band weighting to tide gauge selection and regard the arguments of M09 as further support of our selection of this weighting scheme.

5. Discussion and Conclusion

[50] Accurate observations of sea level change are critical to understanding how changes in climate affect the Earth's water reservoirs. However, those same observations will also determine the socioeconomic impact of sea level change. Although the public is justifiably concerned about the future of sea level rise, estimating future sea change will be difficult absent an understanding of how the current state of the oceans compares with past states. The more challenging work of reconstructing sea levels is still in its infancy, despite well-established reconstructions and studies for SST data. Reconstruction techniques take advantage of both the accurate measurements of modern instruments and the long duration of historical records to investigate how sea level and climate have changed over the past century. Using a fully reconstructed sea level data set, we can study the change in ocean signals (such as those related to the annual cycle and ENSO) over a longer period that cannot be resolved with satellite altimetry records and shorter-duration reconstructions. While the annual and ENSO signals are of interest, investigating climate signals at decadal and multidecadal time scales is even more important because of their potentially significant impact on sea level change.

[51] The work of Ch02 and CW has helped transition the reconstruction techniques of SST into techniques for reconstructing SSH. There is clearly room, however, for improvement. EOFs are simple to compute from satellite altimetry, but are not entirely suitable as basis functions for a reconstruction. EOFs enforce stationarity of the spatial pattern on the resulting reconstruction. We can lessen the impact of stationarity assumptions by using CSEOFs while also capturing the cyclostationary signals in the ocean. The CSEOF loading vectors are periodic with a certain nested

period, defined to be 1 year when attempting to extract the annual cycle signal. Perhaps the greatest advantage in using CSEOFs over EOFs is the ability to capture the evolution of cyclostationary geophysical signals in a single mode.

[52] Past reconstructions have removed the annual cycle signals from both the satellite altimetry and tide gauge data prior to performing the analysis, in part because of the spreading of annual cycle signals across several EOF modes. CSEOF decomposition, on the other hand, separates the annual cycle (Figure 2), capturing the annual cycle as well as its lower-frequency amplitude modulation. The second mode obtained from a CSEOF decomposition of the satellite altimetry data represents the ENSO variability in the data set (Figure 3) with no apparent leakage from the annual cycle signal. Initial CSEOF reconstructions demonstrate an improvement in the correlation of ENSO-reconstructed amplitude and common climate indices from 0.78 to 0.91 when compared with the results reported by CW. Reconstructing individual modes that are dynamically important benefits the evaluation of GMSL and climate indices.

[53] In addition to the choice of basis functions, the weighting used in the reconstruction procedure and the selection of tide gauges has considerable effect on the reconstruction. The choices made by CW provide for a reconstructed data set, but questions remain whether it is the most accurate reconstruction possible. M09 provides justification and support for adopting a latitude-band weighting scheme, and the CSEOF reconstruction computed using such a scheme exhibits good agreement with other sea level data sets. Furthermore, sensitivity tests lead to the conclusion that the reconstruction of signals, such as MAC and ENSO signals, is robust to both the tide gauge selection and weighting scheme. Estimates of GMSL, on the other hand, appear to be sensitive to the tide gauges used in the reconstruction, which is at least partially an artifact of the weighting scheme used.

[54] The procedure of reconstructing sea level does not lend itself well to estimating GMSL. There is no basis function calculated from the short altimetric record, either EOF or CSEOF, that captures and explains mean sea level from 1950 to 2010. One way to address this issue is to introduce an artificial basis function, as done by CW. Alternatively, we choose to decouple the estimate of GMSL from the fitting of the basis functions to the tide gauges. This provides reasonable values for the trend in GMSL. However, these estimates are sensitive to the tide gauge selection particularly when the latitude-band weighting scheme is implemented. In short, incorporating GMSL into sea level reconstructions is not a trivial task and demands further consideration. Despite this fact, the CSEOF reconstruction technique has shown great promise to accurately capture signals in the ocean and provides a viable and robust computational option for improving on earlier published sea level reconstructions.

[55] The reconstructed sea level data set described in this paper is potentially a valuable resource for oceanographers, glaciologists, hydrologists, and climate modelers, and we plan to submit the data set to NASA/JPL PO.DAAC for general release to the Earth system science community.

[56] **Acknowledgments.** This work was supported by NASA Ocean Surface Topography Mission Science Team grants NNX08AR60G and NNX08AR48G and NASA ROSES grant NNX11AE26G. Ocean Topography Project Scientist support for R.R.L. by the NASA/JPL PO.DAAC is gratefully acknowledged. W.H. is supported by NSF CAREER award OCE 0847605 and NASA OSTST award NNX08AR62G. K.Y.K. acknowledges support by the Ministry of Land, Transport, and Maritime Affairs (Ocean Climate Variability Program). The altimeter products used in this study were produced by Ssalto/Duacs and distributed by AVISO, with support from the Centre National d'Etudes Spatiales (CNES). NCEP Reanalysis data were provided by NOAA/OAR/ESRL PSD, Boulder, Colorado, USA, from their website at http://www.esrl.noaa.gov/psd/.

References

Ashok, K., S. K. Behera, S. A. Rao, H. Wang, and T. Yamagata (2007), El Niño Modoki and its possible teleconnection, *J. Geophys. Res.*, *112*, C11007, doi:10.1029/2006JC003798.

Beckley, B. D., F. G. Lemoine, S. B. Lutchke, R. D. Ray, and N. P. Zelensky (2007), A reassessment of global and regional mean sea level trends from TOPEX and Jason-1 altimetry based on revised reference frame and orbits, *Geophys. Res. Lett.*, *34*, L14608, doi:10.1029/2007GL030002.

Berge-Nguyen, M., A. Cazenave, A. Lombard, W. Llovel, J. Viarre, and J. F. Cretaux (2008), Reconstruction of past decades sea level using thermosteric sea level, tide gauge, satellite altimetry, and ocean reanalysis data, *Global Planet. Change*, *62*, 1–13, doi:10.1016/j.gloplacha.2007.11.007.

Calafat, F. M., D. Gomis, and M. Marcos (2009), Comparison of Mediterranean sea level fields for the period 1961–2000 as given by a data reconstruction and a 3D model, *Global Planet. Change*, *68*, 175–184.

Cazenave, A., and R. S. Nerem (2004), Present day sea level change: Observations and causes, *Rev. Geophys.*, *42*, RG3001, doi:10.1029/2003RG000139.

Chambers, D. P., C. A. Melhaff, T. J. Urban, D. Fuji, and R. S. Nerem (2002), Low-frequency variations in global mean sea level: 1950–2000, *J. Geophys. Res.*, *107*(C4), 3026, doi:10.1029/2001JC001089.

Christiansen, B., T. Schmith, and P. Thejll (2010), A surrogate ensemble study of sea level reconstructions, *J. Clim.*, *23*, 4306–4326, doi:10.1175/2010JCLI3014.1.

Church, J. A., and N. J. White (2006), A 20th century acceleration in global sea-level rise, *Geophys. Res. Lett.*, *33*, L01602, doi:10.1029/2005GL024826.

Church, J. A., N. J. White, R. Coleman, K. Layback, and J. X. Mitrovica (2004), Estimates of the regional distribution of sea level rise over the 1950–2000 period, *J. Clim.*, *17*, 2609–2625, doi:10.1175/1520-0442(2004)017<2609:EOTRDO>2.0.CO;2.

Compo, G. P., and P. D. Sardeshmukh (2010), Removing ENSO-related variations from the climate record, *J. Clim.*, *23*, 1957–1978, doi:10.1175/2009JCLI2735.1.

Douglas, B. C. (1991), Global sea level rise, *J. Geophys. Res.*, *96*(C4), 6981–6992, doi:10.1029/91JC00064.

Goswami, B. (1995), A multi-scale interaction model for the origin of the tropospheric QBO, *J. Clim.*, *8*, 524–534, doi:10.1175/1520-0442(1995)008<0524:AMIMFT>2.0.CO;2.

Gröger, M., and H. P. Plag (1993), Estimations of a global sea level trend: Limitations from the structure of the PSMSL global sea level data set, *Global Planet. Change*, *8*, 161–179, doi:10.1016/0921-8181(93)90023-H.

Hamlington, B. D., R. R. Leben, R. S. Nerem, and K.-Y. Kim (2011), The effect of signal-to-noise ratio on the study of sea level trends, *J. Clim.*, *24*, 1396–1408, doi:10.1175/2010JCLI3531.1.

Han, W., et al. (2010), Patterns of Indian Ocean sea level change in a warming climate, *Nat. Geosci.*, *3*, 546–550, doi:10.1038/ngeo901.

Kaplan, A. M., M. A. Cane, Y. Kushnir, A. C. Clement, M. B. Blumenthal, and B. Rajagopalan (1998), Analyses of global sea surface temperature 1856–1991, *J. Geophys. Res.*, *103*(C9), 18,567–18,589, doi:10.1029/97JC01736.

Kaplan, A. M., Y. Kushnir, and M. A. Cane (2000), Reduced space optimal interpolation of historical marine sea level pressure 1854–1992, *J. Clim.*, *13*, 2987–3002, doi:10.1175/1520-0442(2000)013<2987:RSOIOH>2.0.CO;2.

Kim, K.-Y., and C. Chung (2001), On the evolution of the annual cycle in the tropical Pacific, *J. Clim.*, *14*, 991–994, doi:10.1175/1520-0442(2001)014<0991:OTEOTA>2.0.CO;2.

Kim, K.-Y., and G. R. North (1997), EOFs of harmonizable cyclostationary processes, *J. Atmos. Sci.*, *54*, 2416–2427, doi:10.1175/1520-0469(1997)054<2416:EOHCP>2.0.CO;2.

Kim, K.-Y., and Q. Wu (1999), A comparison of study of EOF techniques: Analysis of nonstationary data with periodic statistics, *J. Clim.*, *12*, 185–199, doi:10.1175/1520-0442-12.1.185.

Kim, K.-Y., G. R. North, and J. Huang (1996), EOFs of one-dimensional cyclostationary time series: Computations, examples, and stochastic

modeling, *J. Atmos. Sci.*, *53*, 1007–1017, doi:10.1175/1520-0469(1996)053<1007:EOODCT>2.0.CO;2.

Leuliette, E. W., R. S. Nerem, and G. T. Mitchum (2004), Results of TOPEX/Poseidon and Jason calibration to construct a continuous record of mean sea level, *Mar. Geod.*, *27*, 79–94, doi:10.1080/01490410490465193.

Llovel, W., A. Cazenave, P. Rogel, A. Lombard, and M. B. Nguyen (2009), Two-dimensional reconstruction of past sea level (1950–2003) from tide gauge data and an ocean general circulation model, *Clim. Past*, *5*, 217–227, doi:10.5194/cp-5-217-2009.

Merrifield, M. A., S. T. Merrifield, and G. T. Mitchum (2009), An anomalous recent acceleration of global sea level rise, *J. Clim.*, *22*, 5772–5781, doi:10.1175/2009JCLI2985.1.

Miller, L., and B. C. Douglas (2007), Gyre-scale atmospheric pressure variations and their relation to 19th and 20th century sea level rise, *Geophys. Res. Lett.*, *34*, L16602, doi:10.1029/2007GL030862.

Nerem, R. S. (1995), Global mean sea level variations from TOPEX/POSEIDON altimeter data, *Science*, *268*, 708–710, doi:10.1126/science.268.5211.708.

Nerem, R. S., D. P. Chambers, B. D. Hamlington, R. R. Leben, G. T. Mitchum, T. Phillips, and J. K. Willis (2010), Observations of recent sea level change, paper presented at the IPCC Workshop on Sea Level Rise and Ice Sheet Instabilities, Intergov. Panel on Clim. Change, Malaysia, June.

North, G. R. (1984), Empirical orthogonal functions and normal modes, *J. Atmos. Sci.*, *41*, 879–887, doi:10.1175/1520-0469(1984)041<0879:EOFANM>2.0.CO;2.

Philander, S. G. (1990), *El Niño, La Nina, and the Southern Oscillation*, 293 pp., Academic, San Diego, Calif.

Rasmusson, E. M., and J. M. Wallace (1993), Meteorological aspects of El Niño/Southern Oscillation, *Science*, *220*, 1195–1202.

Rasmusson, E. M., X. Wang, and C. F. Ropelewski (1990), The biennial component of ENSO variability, *J. Mar. Syst.*, *1*, 71–96, doi:10.1016/0924-7963(90)90153-2.

Smith, T. M., R. W. Reynolds, R. E. Livezey, and D. C. Stokes (1996), Reconstruction of historical sea surface temperatures using empirical orthogonal functions, *J. Clim.*, *9*, 1403–1420, doi:10.1175/1520-0442(1996)009<1403:ROHSST>2.0.CO;2.

Tai, C. K. (1989), Accuracy assessment of widely used orbit error approximations in satellite altimetry, *J. Atmos. Oceanic Technol.*, *6*, 147–150, doi:10.1175/1520-0426(1989)006<0147:AAOWUO>2.0.CO;2.

Trenberth, K. E., D. P. Stepaniak, and L. Smith (2005), Interannual variability of patterns of atmospheric mass distribution, *J. Clim.*, *18*, 2812–2825, doi:10.1175/JCLI3333.1.

Vermeer, M., and S. Rahmstorf (2009), Global sea level linked to global temperature, *Proc. Natl. Acad. Sci. U. S. A.*, *106*, 21,527–21,532, doi:10.1073/pnas.0907765106.

Wolter, K. (2010), Multivariate ENSO index, NOAA Earth Syst. Res. Lab., Boulder, Colo. (Available at http://www.esrl.noaa.gov/psd/people/klaus.wolter/MEI/.)

Wolter, K., and M. S. Timlin (1998), Measuring the strength of ENSO events—How does 1997/98 rank?, *Weather*, *53*, 315–324.

B. D. Hamlington, R. R. Leben, and R. S. Nerem, Colorado Center for Astrodynamics Research, Department of Aerospace Engineering Sciences, University of Colorado at Boulder, ECNT 320, 431 UCB, Boulder, CO 80309-0431, USA. (hamlingt@colorado.edu)

W. Han, Department of Atmospheric and Oceanic Sciences, University of Colorado at Boulder, 311 UCB, Folsom Stadium Room 255, Gate 7, Boulder, CO 80309-0311, USA.

K.-Y. Kim, School of Earth and Environmental Science, Seoul National University, San 56-1, Shillim-dong, Gwanak-gu, Seoul 151-747, South Korea.